

# Polyethylene: Structure, Morphology, Molecular Motion and Dielectric Behavior

**Dilip K. Das-Gupta**

*School of Electronic Engineering and Computer Systems  
University of Wales*

## Introduction

**M**acromolecular polymers are viscoelastic materials that can possess the properties of viscous liquid, elastic rubber, or glassy substances, depending on the temperature. For example, a polymer may be glassy at low temperatures, rubber-like at higher temperatures and viscous liquid at still higher temperatures. The unique properties of macromolecular polymers are attributed to their long chain structure. Linear polymers, such as polyethylene, are thermoplastics, which can be remolded many times and have a degree of solubility. Cross-linked polymers are thermoset materials, which cannot be reprocessed and are insoluble. The interaction between the molecular chains, the flexibility of chains, and the spacing of polar groups affect the mechanical properties of polymers. In macromolecules, the flexibility of chains arises from a rotational motion around chain bonds. Crystalline polymers with high molecular weight are hard materials; the linear crystalline region provides strength while the branching provides toughness. The elasticity depends on the ability of the disordered chain segments to stretch under the influence of stress. For electrical insulation application, a large band gap ( $E_g$ ), a low dielectric constant ( $E_r$ ), and a low dielectric loss over a wide frequency range are desirable.

The present paper discusses briefly the morphology, crystal structure, molecular motion and dielectric properties of polymers, particularly polyethylene, which is being increasingly used in wire covering and high voltage cable insulation. Table I provides some of the relevant properties of a few thermoplastic materials [1]. By no means is this a review paper, and the discussion is at a general level. Its aim has been to stress the importance of the basic concepts in molecular motion and the di-

*Linear polymers, such as polyethylene, are thermoplastics, which can be remolded many times and have a degree of solubility.*

**Table I. Properties of a few thermoplastic materials. [1]**

Property	Materials					
	LDPE	HDPE	XLPE	HARD PVC	SOFT PVC	PTFE
Breakdown field $E_b$ (kV/mm)	75	100	50	30	10	25
Dielectric constant $E_r$	~2.3	2.3	2.4	2.3	5.5	2.1
Volume resistivity $\rho$ (Ohm-cm)	$5 \times 10^{17}$	$5 \times 10^{17}$	$\sim 10^{16}$	$10^{15}$	$10^{14}$	$10^{17}$
$\tan \delta$ at 1 MHz	$2 \times 10^{-4}$	$10^{-3}$	$10^{-3}$	$2 \times 10^{-2}$	$10^{-1}$	$10^{-4}$
Density ( $\text{g/cm}^3$ )	0.92	0.95	0.92	1.4	1.2 to 1.3	2.15
Thermal conductivity ( $\text{W/k-m}$ )	0.3	0.4	0.3	0.17	0.17	0.25
Linear thermal expansion coefficient ( $\times 10^{-6}/\text{k}$ )	320	150	320	70	190	120
Tensile strength ( $\text{N/mm}^2$ )	12	15	20	50	15-30	20
Bending strength $\text{N/mm}^2$	15	30	-	100	-	15
E-Modulus $\text{kN/mm}^2$	0.15	0.7	0.1	3	0.05	0.5

0883-7554/94/\$4.00©1994

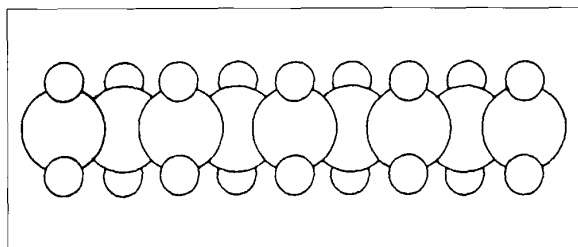


Fig. 1. Molecular structure of polyethylene; C: large circle; H: small circle [2]

electric properties of polymers that are used in electrical insulation.

## Molecular Structure of Polymers

The molecular structure of polyethylene may be represented simply as  $(CH_2)_n$  where  $n$  is very large and its relative molecular mass  $M$ , is given by

$$M = 14.02n + 2.02 \quad (1)$$

$M \approx 14.02n$  when  $n$  is very large

A polyethylene specimen may contain individual chains of different lengths, i.e.,  $n$  is not constant. A polymer system in which all molecules have the same chain length and molecular mass is called "mono disperse." The relative molecular mass of a polymer affects its flow and mechanical properties. In a coplanar conformation, a polyethylene chain containing 1000 carbon atoms, the end-to-end distance will be  $0.13 \mu m$  [2], the C-C bond length and C-C-C bond angle being  $154 \times 10^{-12} m$  and  $109.5^\circ$  respectively. In the liquid state, the kinetic energy of a polymer molecule may provide translational motion of the molecule as a whole, rotation of parts of the molecule, or individual bond vibrations, which can produce conformational changes. However, in the solid state, molecular motions will be restricted, although impeded rotational motions may still occur subject to the availability of sufficient kinetic energy. Fig. 1 shows schematically the atomic configuration of a small length of polyethylene chain, and a diagrammatic representation of chain folding is shown in Fig. 2 [3].

The chain bending is necessary to accommodate long chains within the crystal entity, and it is associated with all lamellar single crystals as shown in Fig. 3 [4]. The lateral dimensions of a polyethylene lamella are of the order of  $10 - 20 \times 10^{-6} m$  with a thickness of only  $10 \times 10^{-9} m$ . The chain axis (i.e.,  $c$ -axis) of the molecule is approximately normal to the plane of the lamella, although the thickness of the lamella is considerably less than the chain. Such an arrangement also conforms to the concept of the chain folding. It has been suggested

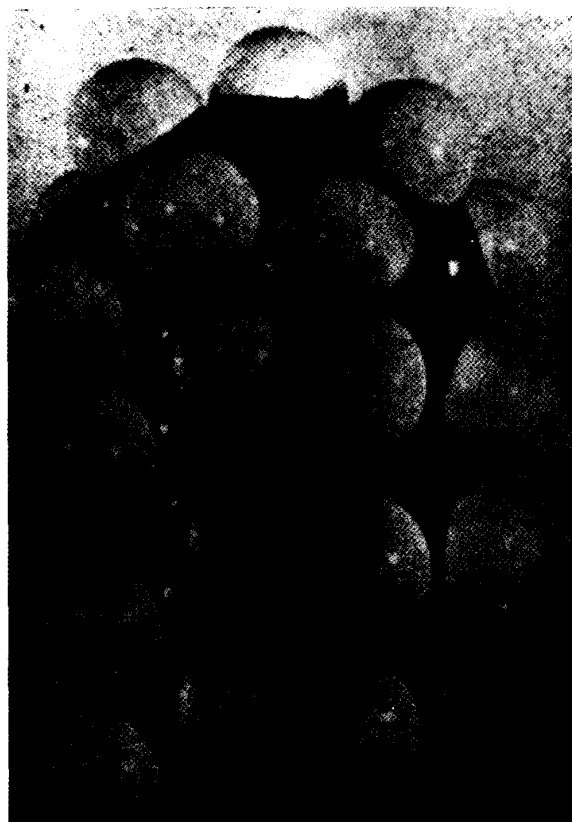


Fig. 2. Schematic representation of chain folding [3]

that the mechanism of a chain refolding may involve a simultaneous displacement of all the chains in the same direction in a cooperative manner, occurring at a sufficiently high temperature [3]. It should be noted that a polymer chain, subjected to an extensional flow during crystallization, can align in the direction of flow, resulting in a fibrillar structure with extended chain crystals in which the chains will be aligned parallel to one another over long distances. For such a case, the chain folding will be minimal. The polymer chains, which form crystallites, are often arranged to form larger ag-

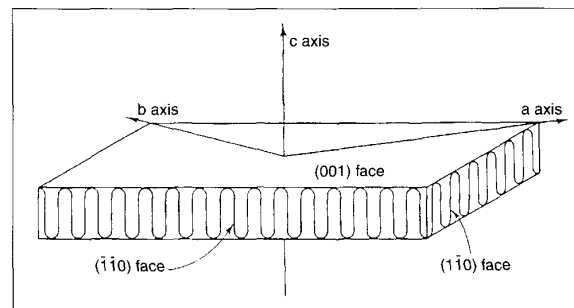


Fig. 3. Chain folded structure of polyethylene crystal [4]

gregates, called spherulites, which grow radially from their nucleation centers until they approach other spherulites. These spherulites are typically  $10^{-5}$  m in diameter [5] and show a "Maltese Cross" pattern when viewed through crossed polarizers (see Fig. 4).

The spherulitic nature together with a model of folded chain crystallite lamellae and the interlamellar amorphous regions tying the lamellae together in a polymer bulk is shown in Fig. 5 [6].

The orthorhombic crystal structure of polyethylene with  $P_{nam}$  symmetry is shown in Fig. 6 [3], in which the chains are of a planar zigzag formation of carbon atoms, with a-, b- and c- axial parameters being 7.368 Å, 4.936 Å, and 2.5405 Å respectively.

Fig. 7 shows a typical X-ray diffraction pattern for semicrystalline polyethylene containing both crystalline and amorphous regions [7]. It may be observed that the two crystalline peaks (110) and (220) are superimposed. The shape of the amorphous peak as well as those of the (110) and (200) peaks were determined using the symmetry rules, and these are shown by areas  $a$ ,  $b$  and  $c$  in Fig. 6 (broken lines).

The amorphous content percentage is given by,

$$\text{Amorphous content \%} = \frac{100xa}{xa + yb + zc} \quad (2)$$

where  $x$ ,  $y$  and  $z$  are derivable correction factors, and  $a$ ,  $b$  and  $c$  are areas mentioned above. The crystal sizes may be obtained from the observed integral breadth, which is defined by,

$$\beta = \frac{\int I(s)ds}{I_{s=0}} \quad (3)$$

where  $I$  is the X-ray intensity for a given value of  $S$  and  $S = 2\theta - 2\theta_{\max}$  where  $2\theta_{\max}$  refers to the scattering angle

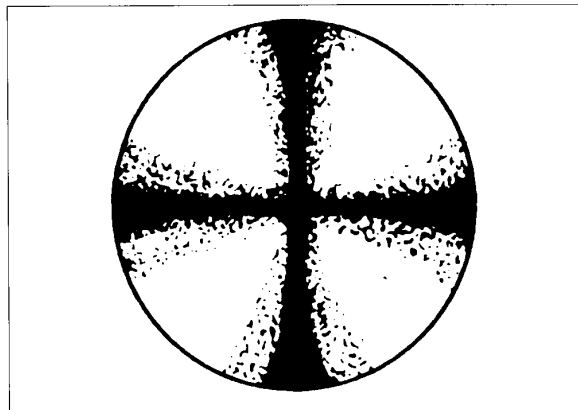


Fig. 4. "Maltese Cross" appearance of spherulites viewed between crossed polarizers [5]

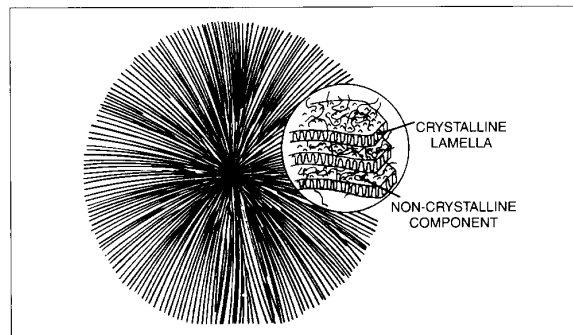


Fig. 5. Schematic diagram of spherulitic morphology in semicrystalline polyethylene. Molecular chain axis is approximately perpendicular to the lamella [6]

at the peak of the curve.  $\beta$  is then related to the crystallite size by,

$$\beta = \frac{k\lambda}{t \cos\theta} \quad (4)$$

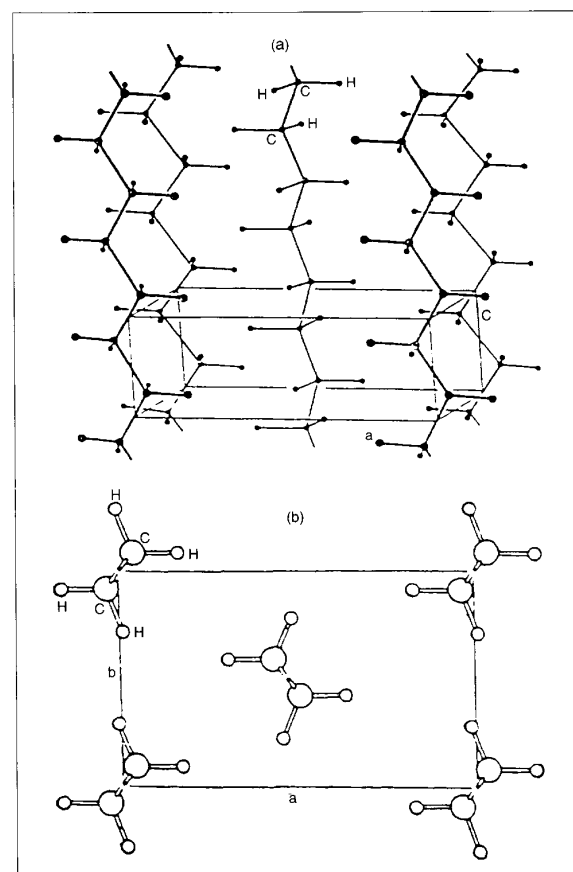


Fig. 6. Crystal structure of polyethylene. (a) General view; (b) Projection along c-axis, i.e. chain direction [3]. Unit cell parameters:  $a = 7.368$  Å,  $b = 4.936$  Å and  $c = 2.547$  Å

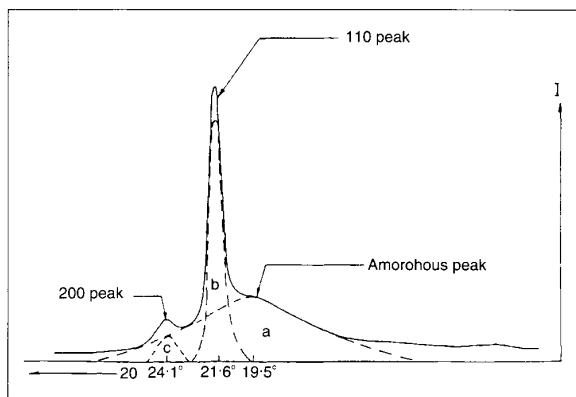


Fig. 7. Continuous line: a typical X-ray diffraction spectrum of polyethylene. Broken line: the resolved diffractometer trace after allowance for background [7]

where  $k$  is a constant,  $\lambda$  the wavelength of the X-rays,  $\theta$  the Bragg angle and  $t$  the edge length of the crystallite. The crystallite size  $t$ , was observed to be 224 Å [7] for this case. Table II gives a list of Bragg angles for different crystal planes. As the crystalline region will have a higher packing efficiency of the molecular chains than in the amorphous area, the crystallites will have a higher density. Polymer density is indeed a good measure of its crystallinity. For example, HDPE with a density of 0.97 g/cm<sup>3</sup> is ~95% crystalline whereas LDPE with a density of 0.915 g/cm<sup>3</sup> is ~60% crystalline. An

Table II. A comparison of theoretical and experimentally observed values of  $2\theta$  for different crystallographic planes of polyethylene.

[Note: Bragg equation,  $\lambda = 2d_{hkl} \sin \theta$ ].

Plane designation (hkl)	Calculated Bragg angle ( $2\theta$ )	Observed Bragg angle ( $2\theta$ ) for crystalline and polyethylene
(110)	21.65	21.65
(200)	24.14	24.15
(210)	30.24	-
(020)	36.37	-
(011)	39.79	39.85
(111)	41.70	41.80
(220)	44.13	44.67
(201)	43.14	43.15
(211)	47.08	47.05
(121)	53.10	-
(321)	64.80	65.10

increase in crystallinity can enhance the mechanical strength and rigidity of the polymer.

The optical transmission through polymers is also affected by the degree of crystallinity. The crystalline region, being denser, will have a higher refractive index and will be less translucent than the amorphous phase. In general, transparent polymers are amorphous, but the converse may not be true, as a lack of transparency may also be caused by the fillers. Furthermore, polymers with very small sizes of crystallites and a low degree of crystallinity may be transparent.

## Molecular Motion in Polymers

Long chain polymers tend to resist changes in bond angles along their backbones and the separation of the individual atoms. The extent of molecular mobility will be temperature dependent. At temperatures close to the absolute zero, a solid polymer will have very little thermal energy and its molecular chain will be stationary. Each possible mode of molecular motion, i.e., motion of branch points, rotation of side groups, crankshaft motion, segmental motion, and motion of crystallite features, requires, of course, a threshold temperature for the activation process. As the temperature increases, the acquired thermal energy is shared by all the possible modes of molecular motions. A rotation around a C-C bond requires only a low potential threshold and is consistent with the concept of free volume activation requiring small energy. This mechanism, known as "crankshaft motion" is shown schematically in Fig. 8, in which the bonds 1 and 7 remain colinear, while the intervening groups move as crankshafts. This is a local motion of the segment of the main chain. This motion has been attributed to the  $\beta$ -relaxation in polyvinyl chloride where the dipolar group, which is attached to the main chain, would not be able to move independently of the polymer backbone.

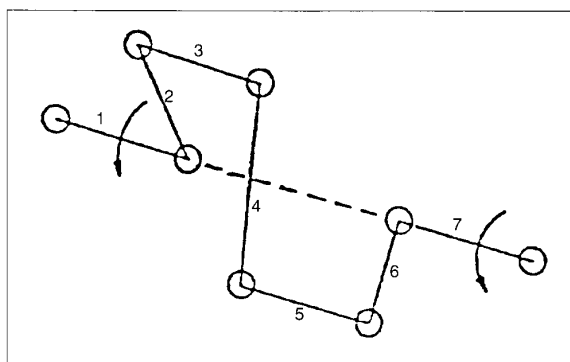


Fig. 8. "Crankshaft" motion of a segment of a molecular chain

A C-C bond, in general, has a rotational potential. A kink jump model has been suggested as being responsible for molecular relaxation at a low temperature ( $\gamma$ -relaxation). In this kink jump model, two gauche positions are exchanged. The trans-gauche potential threshold is 11.5 kJ/mol for polyethylene, and twice the threshold potential (i.e. 23.0 kJ/mol) is required for a kink jump. This value of energy agrees well with the value of 26.0 kJ/mol for the  $\gamma$ -relaxation of polyethylene. Fig. 9 shows the nature of kink site changes [8]. The kink motion resembles the "crankshaft" mechanism. Amorphous and semicrystalline solid polymers exhibit a glass transition temperature,  $T_g$ . Above  $T_g$  large-scale backbone movement of the neighboring molecular chains can occur. Below  $T_g$  the free volume decreases and the segmental motion becomes difficult and extremely slow. However, the "crankshaft" rotations of the main chain involving three to five bonds and rotations of the side group or parts of the side group can occur. The relaxation behavior at  $T_g$  is commonly labeled as primary or  $\alpha$ -process. The main modes of molecular motions of polymers are shown in Fig. 10 [2], from which it may be observed that  $\alpha$ -,  $\beta$ - and  $\gamma$ -relaxations occur in the order of decreasing transition temperatures  $T_\alpha > T_\beta > T_\gamma$ .

When a mechanical stress (tensile or shear stress) is applied to a macromolecular polymer, conformational changes corresponding to a "retarded elastic" behavior occur. These changes are not instantaneous, nor is the recovery when the stress is removed. Simple phenomenological models, viz., the Maxwell model and the

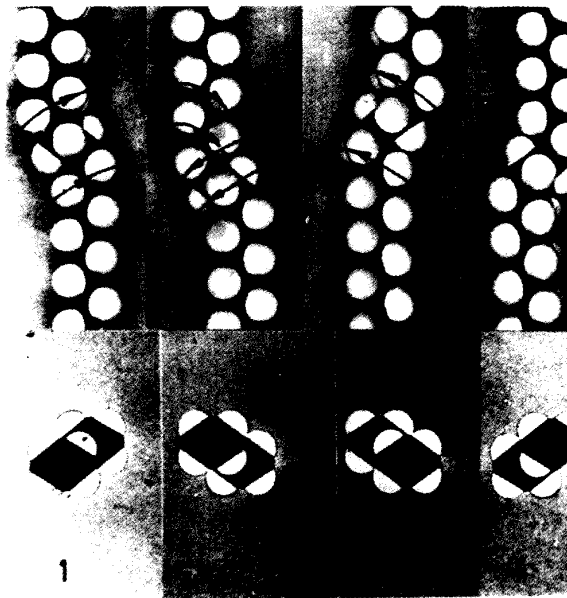


Fig. 9. Kink site changes in a molecular model of polyethylene; 1  $\rightarrow$  2, 3  $\rightarrow$  4, Kink steps and 2-3 Kink jumps [8]

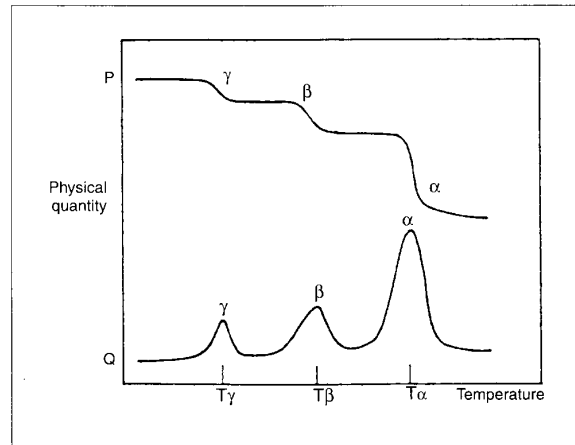


Fig. 10. Schematic diagram of temperature dependent complex properties of polymers including molecular motions, mechanical shear modulus, dielectric permittivity and refractive index which have real and imaginary components [2]

Kelvin Voigt model, based on elastic springs and viscous damping, have been employed to describe the creep and relaxation behavior of polymers. Maxwell's model in its simplest form consists of a single spring attached in series to a damping cylinder. In this model, the frequency-dependent complex shear modulus  $G^*(\omega)$  and its real and imaginary components  $G'(\omega)$  and  $G''(\omega)$  respectively, are given by [8].

$$G^*(\omega) = \frac{i\omega\eta_i}{1+i\omega\tau_i} \text{ with } \tau_i = \eta_i/G_i \quad (5)$$

$$G'(\omega) = G_i \frac{\omega^2\tau_i^2}{1+\omega^2\tau_i^2} \quad (6)$$

$$G''(\omega) = G_i \frac{\omega\tau_i}{1+\omega^2\tau_i^2} \quad (7)$$

$$\text{and } \tan\delta = 1/\omega\tau_i = \text{loss factor} \quad (8)$$

where  $\eta$  is the shear viscosity and  $\tau$  is the relaxation time. These equations resemble the corresponding frequency-dependent dielectric loss process with a series combination of an RC circuit providing an ideal Debye process, R and C being nondissipative resistance and capacitance, respectively.

The Kelvin-Voigt model differs from that of Maxwell in that the damping cylinder is connected in parallel with the spring, i.e., it is analogous to a parallel connection of R and C. For this case, the complex shear modulus  $G^*(\omega)$  and the complex shear compliance  $I^*(\omega)$  are related thus [8]:

$$J^*(\omega) = 1/G^* \quad (9)$$

$$J'(\omega) = \frac{J_i}{1+\omega^2\tau_i^2} \quad (10)$$

$$J''(\omega) = J_i \frac{\omega\tau_i}{1+\omega^2\tau_i^2} \quad (11)$$

$$\text{and } \tan\delta = \omega\tau_i \quad (12)$$

However, these two models are unable to describe the molecular behavior of real macromolecular systems. For example, Maxwell's model cannot explain the time-dependent behavior of creep, and the Kelvin-Voigt model is unable to account for the behavior of stress relaxation. In addition, there is a broad spectrum of relaxation and retardation times in real viscoelastic materials. In order to explain the occurrence of broad relaxation behavior, these two models have been further developed to include an infinite number of discrete elements that can provide continuous relaxation or retardation spectra (see Fig. 11 and 12). For the generalized Maxwellian model,

$$G(t) = \sum_{i=1}^n G_i e^{-t/\tau_i} \quad (13)$$

Alternatively, for the Kelvin-Voigt model,

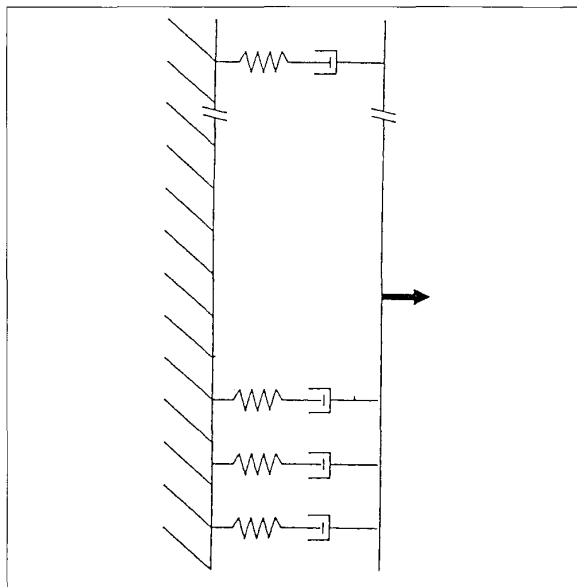


Fig. 11. Generalized Maxwell model with a continuous relaxation or retardation spectra

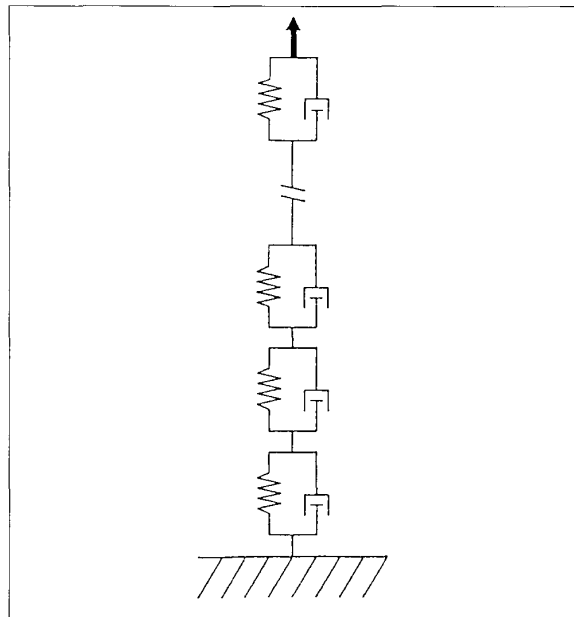


Fig. 12. Generalized Kelvin-Voigt model with a continuous relaxation or retardation spectra

$$J(t) = \sum_{i=1}^n J_i (1 - e^{-t/\tau_i}) \quad (14)$$

where  $n$  is the number of Maxwellian or Kelvin-Voigt elements, each with a discrete relaxation or retardation time  $\tau_i$ . The Maxwellian elements,  $G_i$ , are connected in parallel, whereas the Kelvin-Voigt elements,  $J_i$ , are connected in series, analogous to multiple series connected R-C circuits in parallel arrangements (Fig. 11) and parallel R-C circuits in series arrangements (Fig. 12), respectively. However, both models assume that each discrete relaxation or retardation is an ideal process. These two phenomenological models should be treated with caution.

It has been stated earlier that molecular motions may occur with thermally activated jumps involving molecular segments. On a microscopic level, a change of position in terms of a two-equilibrium, lattice sites potential model in one dimension can explain the polymer relaxation behavior. Using this simple jump model it may be shown that the relaxation time is given by [8].

$$\tau = \frac{1}{2f_0} \exp(E/kT) \quad (15)$$

where  $E$  is the activation energy and  $f_0$  is the jump frequency in a potential trough. Equation 15 is the so-called Arrhenius relationship, which defines the relaxation time as the inverse of the jump rate at a molecular level. It should be noted that it has been shown that the relaxation in elastic and viscoelastic materials

is a cooperative process that is equivalent to the anomalous low frequency dispersion (LFD) in dielectrics containing quasi-free charges [9].

## Dielectric Relaxation in Polymers

If a dielectric is placed in a homogeneous electric field or if a field in the dielectric is produced by introducing a free charge within the material, polarization effects will arise. The electric displacement vector  $D$ , the field vector  $E$ , and polarization vector  $P$ , are related thus,

$$D = \epsilon_0 E + P \quad (16)$$

where  $\epsilon_0$  is the permittivity of free space. It should be noted that  $E$  is the effective average field in the dielectric. The dielectric constant  $\epsilon$ , of a material is defined thus,

$$(D / \epsilon_0 E) = 1 + P/(\epsilon_0 E) \quad (17)$$

$$= 1 + \chi = \epsilon \quad (18)$$

where  $\chi$  is the electric susceptibility. Hence,

$$D = \epsilon_0 \epsilon E \quad (19)$$

The dielectric constant,  $\epsilon$ , varies with the frequency of the applied electric field, and at certain frequencies, energy can be dissipated within the dielectric. The frequency dependence of the dielectric constant has considerable practical importance. For example, dielectric heating in lossy polymers may cause a thermal breakdown.

The dynamic mechanical behavior of a material has been described by the frequency dependence of the complex shear modulus  $G^*(\omega)$  and the complex shear compliance  $J^*(\omega)$ . In a similar manner, the linear response of a dielectric to an ac field is described as the frequency dependence of the complex dielectric constant  $\epsilon^*(\omega)$ , which is expressed thus,

$$\epsilon^*(\omega) = \epsilon'(\omega) - i\epsilon''(\omega) \quad (20)$$

where  $\epsilon'$  and  $\epsilon''$  are the real and imaginary parts of  $\epsilon^*(\omega)$ . The dielectric loss is proportional to the imaginary part of the dielectric constant and it will occur at a frequency centered on  $\omega_0$ . The ratio  $\epsilon''(\omega)/\epsilon'(\omega) = \tan \delta$  is the dielectric loss tangent or the dissipation factor, where  $\delta$  is the phase angle between the electric field and the polarization of the dielectric. In a perfect dielectric the phase angle between the current and voltage is  $\pi/2$ . However, in a real dielectric, the current leads the volt-

age by  $(\pi/2 - \delta)$ . The power factor is expressed by  $\sin \delta$  and  $\epsilon''(\omega) = \epsilon'(\omega) \tan \delta$  is known as the dielectric loss index of the material. The loss tangent of polar polymers are generally much greater than nonpolar polymers. For nonpolar polymers the loss tangent may, however, increase sharply due to a presence of additives, impurity concentrations and physical heterogeneity. The frequency-dependent dielectric constant apparently arises with polar molecules, and the ideal dielectric relaxation behavior may be represented by the following Debye expressions,

$$\epsilon^*(\omega) = \epsilon_\infty + \frac{\epsilon_0 - \epsilon_\infty}{1 + i\omega\tau} \quad (21)$$

$$\epsilon'(\omega) = \epsilon_\infty + \frac{\epsilon_0 - \epsilon_\infty}{1 + (\omega\tau)^2} \quad (22)$$

$$\text{and } \epsilon''(\omega) = \frac{(\epsilon_0 - \epsilon_\infty) \tau}{1 + (\omega\tau)^2} \quad (23)$$

where  $\epsilon_0$  and  $\epsilon_\infty$  are the static (low frequency) and very high frequency dielectric constants respectively. The transition from high to low value of the dielectric constant occurs at  $\omega_p = \tau^{-1}$  where  $\tau$  is the relaxation time of the Debye process. Fig. 13 shows the frequency dependence of the real and imaginary parts of the complex susceptibility of an ideal Debye process corresponding to equations 21 - 24 in a  $\log \chi - \log \omega$  plot. It may be observed that the loss peak has a full width at half height  $\lambda_D = 1.144$  decades, and it is symmetric in the  $\log \omega$  scale [10]. The electrical equivalent circuit for a physically realistic Debye process will consist of an  $R$ - $C$  circuit with an additional capacitor  $C_\infty$  in parallel, which represents the free space permittivity at very high frequency [10]. By eliminating the parameter  $(\omega\tau)$

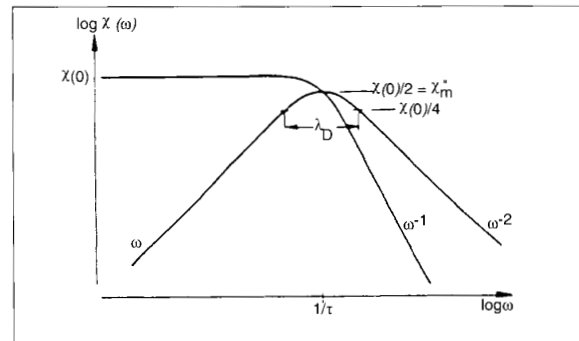


Fig. 13. The frequency dependence of the real and imaginary components of the complex susceptibility for an ideal Debye behavior. The loss peak is symmetric in the  $\log \omega$  scale with  $\lambda_D = 1.144$  decades [10]

in equations 22 and 23, the following expression is obtained,

$$\left(\epsilon' - \frac{\epsilon_0 + \epsilon_\infty}{2}\right)^2 + (\epsilon'')^2 = \left(\frac{\epsilon_0 - \epsilon_\infty}{2}\right)^2 \quad (24)$$

this is the equation of a circle of radius  $(\epsilon_0 - \epsilon_\infty)/2$  and center at  $(\epsilon_0 + \epsilon_\infty)/2$  and a plot of  $\epsilon'$  (or  $\chi'$ ) against  $\epsilon''$  (or  $\chi''$ ) will be a semicircle that is called a Cole-Cole plot [11] and it is shown in Fig. 14 [10]. The applicability of the Debye model may be investigated by comparing the experimentally observed data, when fitted appropriately with the nature of the plots shown in Fig. 13 and 14.

The dielectric behavior of many polar liquids appears to agree well with the Debye process. However, in solid polymers, the dielectric response departs noticeably from the Debye behavior. For such materials, the width of the loss peaks is significantly broader than 1.144 decades, and their peak magnitudes are also lower than the values predicted by the Debye process. In many cases the loss-peaks are also observed to be asymmetric about  $\omega_p$ . In order to account for moderate departures of the dielectric behavior from the Debye response, the following modification to equation 21 was proposed [11].

$$\epsilon^*(\omega) - \epsilon_\infty = \frac{1}{1 + (i\omega\tau)^{1-\alpha}} \quad (25)$$

where  $\alpha$  represents the angle of tilt of the circular arc from the real axis in which the complex plane graph of Fig. 14 is tilted by  $\alpha\pi/2$ . Such a modification has no physical significance. For severe non-Debye forms of dielectric behavior, yet another modification was proposed [12], which is as follows,

$$\epsilon^*(\omega) - \epsilon_\infty = \frac{1}{(1 + i\omega\tau)^{1-\beta}} \quad (26)$$

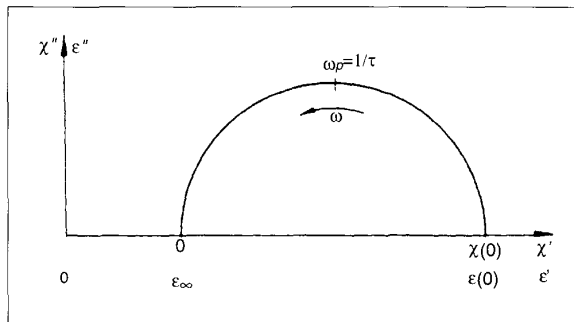


Fig. 14. The complex  $\chi''$  (and  $\epsilon''$ )/ $\chi'$  (and  $\epsilon'$ ) diagram (i.e., Cole-Cole plot) for an ideal Debye response [10]

which gives an asymmetric Cole-Cole plot in which the distorted arc has an angle of tilt to the tangent of the distorted arc of  $(1 - \beta)\pi/2$ . Again, the parameter  $\beta$  has no apparent physical significance. Equations 25 and 26 both describe broad dispersion and invoke the concept of a spread of relaxation times covering a very wide range.

There are many observed dielectric responses of solid materials, including semiconductors, that do not conform with the semiempirical equations 25 and 26. Although a decay function  $\psi$ , of the form [13],

$$\psi = e^{-(t/\tau)^\gamma}, \quad 0 < \gamma \leq 1 \quad (27)$$

appears to provide good agreement with the dielectric responses of many solid polymers, there is no physical explanation for it as yet. The dielectric constant is also a complex function of temperature and for an ideal Debye case, the nature of the exponential temperature dependence of the relaxation time is [10],

$$\chi^*(\omega) \propto \frac{1}{1 + i\omega\tau_\infty \exp(E/kT)} \quad (28)$$

where  $\tau_\infty$  is an appropriate pre-exponential factor and  $E$  is the activation energy. Thus, the susceptibility is the same function of  $\log_e \omega$  as of  $E/kT$ , and a plot of the frequency response of the temperature response should provide the identical loss peaks, which shift to higher temperatures with increasing frequency, or alternatively, to the higher frequencies with increasing temperatures [10]. However, for non-Debye-like dielectric behavior, the frequency dependence and the temperature dependence are not related in an unambiguous manner, and it is usual to plot the frequency dependence at a constant temperature. It has been shown that the frequency dependence of the dielectric loss peaks may be suitably represented by an empirical law combining two power laws, below and above the peak frequency  $\omega_p$ , respectively [10, 14]

$$\chi''(\omega) \propto \frac{1}{(\omega/\omega_p)^{-m} + (\omega/\omega_p)^{1-n}} \quad (29)$$

where  $m$  and  $(1 - n)$  are in the range of 0 to 1 and  $\omega_p$  is generally temperature dependent. It has been claimed that equation 29 can represent the dielectric behavior over a wide range of frequencies, extending to eight to ten decades in many cases. A special case of equation 29 is the ideal Debye behavior when  $m = 1$  and  $1 - n = 1$ . In general, including the hopping of charge carriers, which also give rise to dielectric response, the non-Debye-shaped loss peaks in all dielectric systems obey the 'Universal Law' [9, 10, 14-18]



$$\chi'(\omega) \propto \chi''(\omega) \propto \omega^{-1-n}, \quad \omega > \omega_p \quad (30)$$

$$\chi''(\omega) \propto \chi'(0) - A\chi'(\omega)\alpha\omega^{+m}, \quad \omega < \omega_p \quad (31)$$

where A is a constant and  $\chi(0)$  is the susceptibility at zero frequency. A consequence of the high frequency behavior of equation 30 is that,

$$\chi''(\omega)/\chi'(\omega) = \cot(n\pi/2) \quad (32)$$

which means that the ratio  $\chi''(\omega)/\chi'(\omega)$  is independent of frequency. It has been suggested that the universal relations, stated above, extend from very high frequencies, i.e., below the infrared region, down to the onset of low frequency dispersion in charge carrier dominated systems [10]. It has been proposed that the observed dielectric relaxation phenomena of imperfect materials may be explained by a model of microscopic units, with an array of clusters in a macroscopic structure [19]. The universal relation in time domain, which represents the Fourier transform of the frequency-domain response, is given by the following expression [10],

$$f(t)\alpha I(t) \propto \frac{1}{(\omega_p t)^n + (\omega_p t)^{1+m}} \quad (33)$$

where I represents the discharge current of a real dielectric. Equation 33 provides two straight lines in the logarithmic scale, one at short times with a slope of  $-n$  and another at long times with a slope of  $-1-m$ . The loss-peak frequency is the reciprocal time at which the transition occurs from one process to the other. For an applied step voltage  $V_0$ , the complex dielectric constant  $\epsilon^*(\omega)$  and the discharge current are related thus [20],

$$\epsilon^*(\omega) = \epsilon_\infty + \frac{1}{C_0 V_0} \int I(t) e^{-i\omega t} \alpha \chi dt \quad (34)$$

where  $C_0$  is the geometric capacitance of the sample holder without the sample, (i.e., the vacuum capacitance). The Fourier transformation of equation 34 may be performed numerically or analytically for which the functionality of  $I(t)$  needs to be specified. Using the latter approach, i.e., the Hamon Approximation [21], it may be shown that [10]

$$\chi''(f)_{Hz} = \frac{A}{C_0 V_0} \frac{1}{\pi f} I(1/2\pi f) \quad (35)$$

$$\text{or } \chi''(1/2\pi t)_{Hz} = \frac{a}{C_0 V_0} t I(t) \quad (36)$$

where the parameter A may be adjusted to unity provided the values of the exponents m and n of equation 33 fall within the appropriate range. Thus, the dielectric loss behavior may be identified with a relatively small error from a measurement of the discharge current at very long times and by plotting  $tI(t)$  in a log scale against  $1/2\pi t$ , which then becomes a plot of  $\chi''(f)$  with the appropriate scaling factor  $A/C_0 V_0$ , the parameter A being set to a value between 1 and 1.5. Alternatively, a plot of  $\epsilon''(f)$  may be obtained by using the Hamon approximation in the following form [21],

$$\epsilon''(f) = \frac{I(t)}{2\pi f C_0 V_0} = \frac{I(0.1/f)}{2\pi f C_0 V_0} \quad (37)$$

where f is the Hamon frequency ( $= 0.1/t$ ). This approximation provides good accuracy in the determination of the dielectric loss for non-Debye-like loss behavior. Using this technique, the behavior of the dielectric loss peak in the low frequency range of  $10^{-5}$  Hz to  $10^{-1}$  Hz has been successfully studied for polyethylene terephthalate (PET) and polyvinylidene fluoride (PVDF) [22, 23].

Polyethylene shows  $\alpha$ -,  $\beta$ - and  $\gamma$ - relaxations. A relaxation is dielectrically active only when there is a reorientation of a dipole moment vector and also a release of space charges. Any presence of C=O dipole and polar additives will introduce dipole moments in polyethylene, which may couple the molecular motions of a polymer to the external field. An effective dipole moment of 2.3D was obtained in oxidized polyethylene due to the presence of a C=O group, and it has been suggested that the  $\alpha$ - relaxation arose from carbonyl groups in the crystalline region of polyethylene [25]. Dielectrically active  $\beta$ - and  $\gamma$ - relaxations occur in the disordered regions of polyethylene, the actual dipoles being carbonyl groups as before. Thus, it may be stated that the dielectric relaxations of polyethylene owe their origin to the extraneous carbonyl group and/or other impurity dipoles. The dielectric losses of neutron-irradiated (up to 65 Mrad) cables insulated with hydrocarbon polymers have been studied in the frequency range of  $10^{-4}$  to  $10^{-3}$  Hz at 50°C [26]. The results show that a new relaxation loss peak arises upon irradiation, and it has been attributed to local dipoles that are formed by the irradiation. Dielectric studies at the frequency range of  $10^{-5}$  to  $10^5$  Hz have the advantage that the dielectric loss can be separated from the conductivity from such measurements. The measured loss may be expected to approach asymptotically to a frequency-independent conductance value, whereas the dipolar losses should show complex frequency dependence [26]. Figs. 15 and 16 show the dielectric behavior of unaged and ac-aged (6 kV/mm, 2.5 kHz, 69 hours) low density polyethylene (LDPE) in a 0.1 NaCl solution [27].

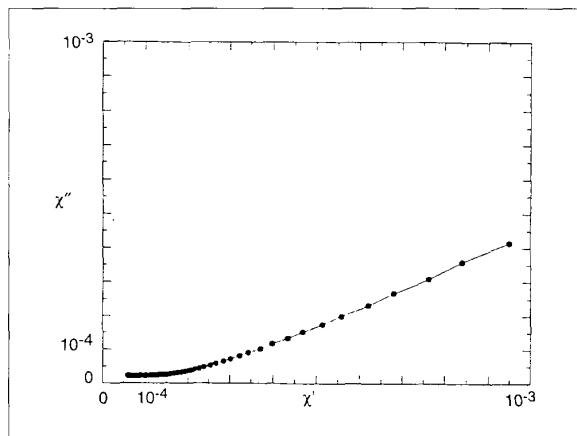


Fig. 15. Dielectric behavior of unaged LDPE sample at RT

The  $\chi''(\omega)/\chi'(\omega)$  plot of the unaged LDPE (Fig. 15) shows a frequency-independent, low flat loss behavior at high frequencies, and this is followed by the low-frequency dispersion process (LFD). The corresponding plot for the aged sample (Fig. 16) exhibits the LFD process for the entire frequency range. These observations also indicate that such dielectric behavior may originate from a movement of slow charge carriers [10], which are probably ions. It is suggested that the dielectric spectroscopy in the frequency range of  $10^5$  Hz to  $10^5$  Hz is a valuable diagnostic method in the assessment of the deterioration of the insulating properties of hydrocarbon polymers under continued electrical stress.

**Dilip K. Das-Gupta** is a reader at the School of Electronic Engineering Science, University of Wales, Bangor, Gwynedd, U.K., where he has worked since 1965. A native of India, he received the B.S. degree in

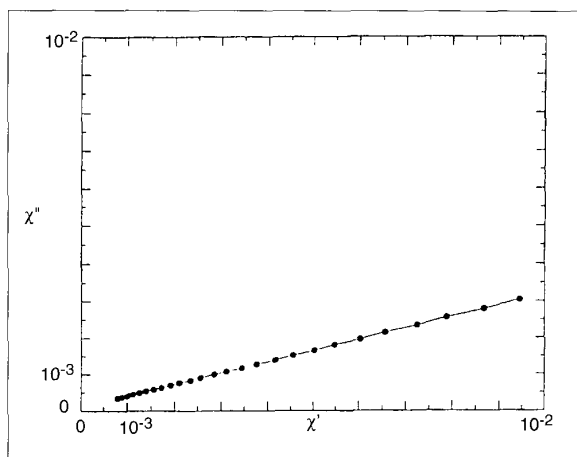


Fig. 16. Dielectric behavior of ac aged (6 kV/mm, 2.5 kHz, 0.1 NaCl, 69 hours) LDPE sample at RT

physics (1st class honors) and the M.Sc. degree in radio physics from the University of Calcutta. In 1949 he emigrated to the U.K., where he worked as an electronics engineer for Pye Ltd., Cambridge, as a research engineer for Elliott Brothers, London, and as deputy chief instrument engineer for The Distillers Co., Ltd., London. He received his Ph.D. in physics in 1960 from the University of London and the D.Sc. degree in electrical materials science in 1989 from the same institution.

Dr. Das-Gupta's academic specialty is in electrical materials science and his primary research interest encompasses high field electrical conduction processes and piezo- and pyroelectric properties of nonpolar and polar insulating polymers. He has published some 65 journal articles on his research. He is a chartered engineer and fellow of the IEE (UK), a senior member of the IEEE and a chartered physicist and fellow of the Institute of Physics (UK). He will receive the 1994 Thomas W. Dakin Award at the International Symposium on Electrical Insulation in Pittsburgh, PA in June, where he will also deliver the Dakin Award Lecture.

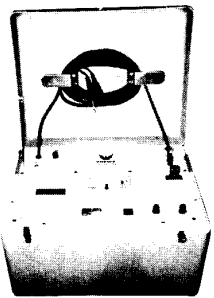
## References

1. D. Kind and H. Karner, *High Voltage Insulation Technology*, Translated from German by Y. N. Rao, Friedr. Vieweg & Son, Braunschweig/Wiesbaden (1985), Appendix 3, pp. 173-175.
2. C. Hall, *Polymer Materials*, Macmillan, London (1989), 2nd ed., Chapters 1-3, pp. 1-54.
3. A. Keller, *Polymer Crystals*, Reports on Progr. in Phys., 31, Part 2 (1968), pp. 623-704.
4. T. Alfrey and E. F. Gurnee, *Organic Polymers*, Prentice-Hall, Englewood Cliffs, N. J. (1967), Chapter 1, pp. 1-20.
5. S. L. Rosen, *Fundamental Principles of Polymeric Materials*, Wiley Interscience, New York (1982), Chapter 5, pp. 37-46.
6. M. G. Broadhurst and G. T. Davis, "Piezo- and Pyroelectric Properties" in *Topics in Applied Physics, Electrets*, ed. G. M. Sessler, Berlin (1979), Chapter 5, pp. 284-319.
7. D. K. Das-Gupta and T. Noon, "Some Spectroscopic and Optical Methods to Characterize Trap Sites in Polyethylene," Inst. Phys. Conf. Ser. No. 27 (1975), Chapter 2, pp. 122-128.
8. U. Eisele, *Introduction to Polymer Physics*, Springer-Verlag, Berlin (1990), Chapter 4, pp. 26-34.
9. R. M. Hill and L. A. Dissado, "Relaxation in Elastic and Viscoelastic Materials," J. Mater. Sci., (1983) 19, pp. 1576-1595.
10. J. K. Jonscher, *Dielectric Relaxation in Solids*, Chelsea Dielectric Press, London (1983) Chapter 3, pp. 62-115, Chapter 5, pp. 161-253 and Chapter 6, pp. 254-293.
11. K. S. Cole and R. H. Cole, "Dispersion and Absorption in Dielectrics: 1. Alternating Current Characteristics," J. Chem. Phys., 9 (1941), pp. 341-351.
12. D. W. Davidson and R. H. Cole, "Dielectric Relaxation in Glycerol, Propylene Glycol and n-Propanol," J. Chem. Phys., 19 (1951), pp. 1484-1490.
13. G. Williams and D. C. Watts, "Non-Symmetrical Dielectric Relaxation Behaviour Arising from a Simple Empirical Decay Function," Trans. Faraday Soc., 66 (1970), pp. 80-91.
14. A. K. Jonscher, "A New Model of Dielectric Loss in Polymers," Colloid & Polym. Sci., 253 (1975), pp. 231-250.

15. R. M. Hill and A. K. Jonscher, "The Dielectric Behaviour of the Condensed Matter and its Many Body Interpretation," *Contemp. Phys.*, **24** (1983), pp. 75-110.
16. L. A. Dissado and R. M. Hill, "Anomalous Low Frequency Dispersion," *J. Chem. Soc., Faraday Trans.*, **2**, **80** (1984), pp. 291-319.
17. A. K. Jonscher, "Admittance Spectroscopy of Systems Showing Low Frequency Dispersion," *Electrochimica Acta*, **35** (1990), pp. 1595-1600.
18. A. K. Jonscher, "Low Frequency Dispersion in Volume and Interfacial Situations," *J. Mater. Sci.*, **26** (1991), pp. 1618-1626.
19. L. A. Dissado and R. M. Hill, "A Cluster Approach to the Structure of Imperfect Materials and Their Relaxation Spectroscopy," *Proc. Roy. Soc. Lond.*, **A390** (1983), pp. 131-180.
20. H. Block, "The Nature and Application of Electrical Phenomena in Polymers" in *Electronic Phenomena in Polymer Science, Advances in Polymer Science*, **33**, (1979), pp. 94-167.
21. B. V. Hamon, "An Approximate Method for Deducing Dielectric Loss Factor from Direct Current Measurement," *Proc. IEE (London)* **99**, Pt. IV (1952), pp. 151-155.
22. D. K. Das-Gupta and K. Joyner, "On the Nature of Absorption Currents in Polyethylene Terephthalate (PET)," *J. Phys. D: Appl. Phys.*, **9** (1976), pp. 829-840.
23. D. K. Das-Gupta, K. Doughty and R. S. Brockley, "Charging and Discharging Currents in Polyvinylidene Fluoride," *J. Phys. D: Appl. Phys.*, **13** (1980), pp. 2101-2104.
24. D. K. Das-Gupta and R. S. Brockley, "A Study of Absorption Currents in Low Density Polyethylene," *J. Phys. D: Appl. Phys.*, **11** (1978), pp. 955-962.
25. M. E. Baird, *Electrical Properties of Polymeric Materials*, The Plastic Institute Monograph (1973).
26. F. I. Mopsik, "Radiation-Induced Dielectric Loss in Hydrocarbon Polymers," *J. Polym. Sci. Pt B: Polym. Phys.*, **31** (1993), pp. 1989-1993.
27. A. Svatik, P. C. Scarpa, D. K. Das-Gupta, D. E. Cooper & C. Raczkowski, "Dielectric Polarization and Relaxation Behaviour of AC Aged Polyethylene with Liquid Electrodes," Annual Report, Conference on Electrical Insulation and Dielectric Phenomena (CEIDP), (1993), pp. 654-659.

**PORTABLE, RUGGED, RELIABLE**

**INSULATION ANALYZER**



Model PM-5A

- Measures applied voltage/current and temperature
- Calculates insulation resistance and polarization index
- Output 500, 1000, 2500, 5000 VDC
- Automatic microprocessor control
- Hard copy printout

**PHENIX**

**TECHNOLOGIES**

Industrial Drive • Accident, Maryland 21520  
Telephone (301) 746-8118 • Fax (301) 895-5570

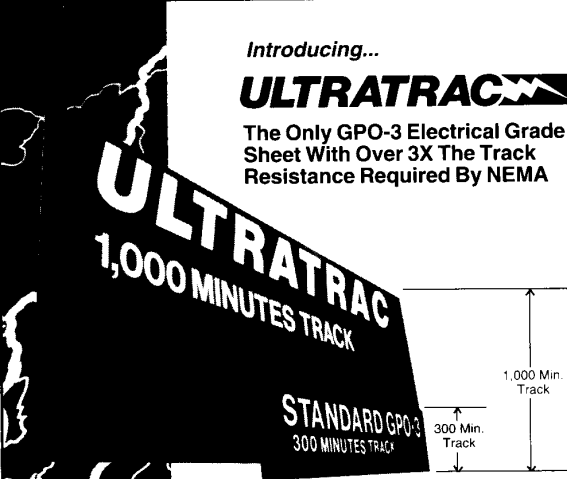
**HIGH VOLTAGE • HIGH CURRENT • HIGH POWER  
TEST SYSTEMS AND COMPONENTS**

Reader Service Number 9

Introducing...

**ULTRATRAC**

The Only GPO-3 Electrical Grade Sheet With Over 3X The Track Resistance Required By NEMA



...At No Extra Cost!

- Only GPO-3 with a specified track resistance of 1,000 minutes.
- Improved flexural strength & arc resistance over standard GPO-3.
- Excellent flame resistance, low smoke generation, non-toxic.

For more information, call 814-868-3691

**haysite** haysite reinforced plastics  
5599 New Perry Highway • Erie, PA 16509  
Phone: (814) 868-3691 • FAX (814) 864-7803  
An Alco Industries Company

Reader Service Number 18